

INCORPORATING SPATIALLY VARYING EFFECTIVE-MASS IN THE WIGNER-POISSON MODEL FOR AIAs/GaAs RESONANT-TUNNELING DIODES

K. K. Gullapalli and D. P. Neikirk
Microelectronics Research Center, MER 1.604 / 79900
The University of Texas at Austin, Austin, TX 78712 (512)-471-8104

Abstract

We present a single band equation of motion for the Wigner function, incorporating the effects of a spatially varying band structure. The transport equation is discrete in position, shedding light into the numerical aspects of the problem. While conventional upwind differencing to approximate the drift term was found adequate for Al_{0.3}Ga_{0.7}As/GaAs devices, it is completely unsatisfactory in modeling AIAs/GaAs resonant-tunneling diodes, particularly when the large change in effective-mass is included. Suggesting a new approach, meaningful steady state conduction curves for AIAs/GaAs diodes are presented for the first time.

Physical Model

With the need for studying effects of the detailed bandstructure such as Γ -X transfer in mind, the band structure is Fourier expanded: $E(k) = \sum_{n=1}^{\infty} (4\hbar^2/n^2 m_n^* a^2) [1 - \cos(nka/2)]$, a being the lattice constant. The Brillouin zone is $[-2\pi/a, 2\pi/a]$. Given that the masses m_n^* are spatially varying, we obtain the following equation of motion for the Wigner function:

$$\begin{aligned} \frac{\partial f}{\partial t} = & - \sum_{n=1}^{\infty} \frac{2\hbar \sin(nka/2)}{n m_n^* a} \left[\frac{f(q+na/4, k) - f(q-na/4, k')}{na/2} \right] + \frac{2}{\pi\hbar} \int dk' f(q, k') V(q, k-k') + \left. \frac{\partial f}{\partial t} \right|_{coll.} \\ & - \sum_{n=1}^{\infty} \frac{4}{n^2} \frac{\hbar}{\pi a^2} \left\{ \int dk' \sin\left(\frac{nk'a}{2}\right) \left[f\left(q + \frac{na}{4}, k'\right) M_n^e\left(q + \frac{na}{4}, k-k'\right) - f\left(q - \frac{na}{4}, k'\right) M_n^e\left(q - \frac{na}{4}, k-k'\right) \right] \right. \\ & \left. + \int dk' \cos\left(\frac{nk'a}{2}\right) \left[f\left(q + \frac{na}{4}, k'\right) M_n^o\left(q + \frac{na}{4}, k-k'\right) + f\left(q - \frac{na}{4}, k'\right) M_n^o\left(q - \frac{na}{4}, k-k'\right) \right] \right\} \\ & + \sum_{n=1}^{\infty} \frac{4}{n^2} \frac{2\hbar}{\pi a^2} \int dk' f(q, k') M_n^o(q, k-k') \end{aligned} \quad (1)$$

where the first line in eq. 1 is the equation of motion if the effective-mass were uniform and

$$M_n^e(q, k) = \int dr \left(\frac{1}{m_n^*(r)} - \frac{1}{m_n^* GaAs} \right) \cos[2k(q-r)], \quad M_n^o(q, k) = \int dr \frac{\sin[2k(q-r)]}{m_n^*(r)}, \quad V(q, k) = \int dr v(r) \sin[2k(q-r)]$$

$v(r)$ includes, in addition to the self-consistent potential, the Γ - Γ offset between the two materials.

Using the "minimal Hermitian form" ($\hat{H} = -(\hbar^2/2) \partial/\partial z (1/m^*) \partial/\partial z + v$) [1] to describe the effects of spatially varying effective-mass is inconsistent with the Weyl transform. By the Weyl correspondence rule, the Hamiltonian in position representation for a parabolic energy band is [2]:

$$\hat{H} = -\frac{\hbar^2}{8} \left[\frac{1}{m^*(z)} \frac{\partial^2}{\partial z^2} + 2 \frac{\partial}{\partial z} \frac{1}{m^*(z)} \frac{\partial}{\partial z} + \frac{\partial^2}{\partial z^2} \frac{1}{m^*(z)} \right] + v(z)$$

The equation of motion for the Wigner function in a parabolic band is just the $a \rightarrow 0$ limit of eq. 1.

Numerical Model

Computational resources limit the numerical treatment to nearest and second nearest neighbor coupling, and hence only two (appropriately chosen) components in eq. 1 can be included. For Γ - Γ tunneling the $n=4$ component is sufficient. The rate of change of the Wigner function $f(q, k)$ being determined only by its values at $q, q+a$, and $q-a$, eq. 1 is solved on the discrete phase-space given by $\{q_j | q_j = j\Delta; j = 1, 2, \dots, N_q\}$ and $\{k_n | k_n = \pi(2n-1-N_k)/(2N_k\Delta); n = 1, 2, \dots, N_k\}$ with $\Delta = a$ (5.6533 Å). We get a set of linear algebraic equations $\sum_{j'n'} L_{jn;j'n'} f_{j'n'} = b_{jn}$ where

$$L_{jn;j'n'} = -\frac{\sin(2k_n\Delta)M_{j'n-n'}^e}{2N_k\Delta} \left(\frac{\delta_{j'j+1} - \delta_{j'j-1}}{2\Delta} \right) - \frac{\cos(2k_n\Delta)M_{j'n-n'}^o}{4N_k} \left(\frac{\delta_{j'j+1} + \delta_{j'j-1}}{\Delta^2} \right) \quad (2)$$

$$+ \frac{M_{j'n-n'}^o + 2V_{j'n-n'}}{N_k} \delta_{j'j} + \frac{\delta_{j'j}}{\tau_f} \left(\frac{f^{eq}}{\sum_{n''} f^{eq}} - \delta_{n'n} \right) + T_{jn;j'n'}$$

and b is the boundary contribution. The resulting matrix equation is solved using block LU factorization. T , the discrete drift term (the first term on the right-hand-side of eq. 1) will be discussed shortly. M^e , M^o and V are evaluated using fast sine and cosine transforms:

$$M_{jn-n'}^e = \frac{(-1)^{n'-n}}{2} \left(\frac{1}{m_{j+N_k/2}^*} + \frac{1}{m_{j-N_k/2}^*} - \frac{2}{m_{GaAs}^*} \right) + \left(\frac{1}{m_j^*} - \frac{1}{m_{GaAs}^*} \right) + \sum_{j'=1}^{N_k/2-1} \left(\frac{1}{m_{j+j'}^*} + \frac{1}{m_{j-j'}^*} - \frac{2}{m_{GaAs}^*} \right) \cos \left[\frac{\pi(n'-n)j'}{N_k/2} \right]$$

$$M_{jn-n'}^o = \sum_{j'=1}^{N_k/2-1} \left(\frac{1}{m_{j+j'}^*} - \frac{1}{m_{j-j'}^*} \right) \sin \left[\frac{\pi(n'-n)j'}{N_k/2} \right], \quad V_{jn-n'} = \sum_{j'=1}^{N_k/2-1} (v_{j+j'} - v_{j-j'}) \sin \left[\frac{\pi(n'-n)j'}{N_k/2} \right]$$

For a parabolic energy band, the drift term appears as the spatial derivative of the Wigner function. It is then suggested that a stable numerical model be obtained by upwind differencing the drift term [1, 3, 4]. Here however, the drift term is already discrete in position. We obtain a numerically stable model by making the following approximation in T :

$$[f(q+\Delta) - f(q-\Delta)] \rightarrow [f(q+\Delta) - f(q-\Delta)] + \delta[f(q+\Delta) - 2f(q) + f(q-\Delta)] \quad (3)$$

where $|\delta| \ll 1$ so that the deviation from eq. 1 is small, and $k\delta < 0$ for stability (upwind bias). When $|\delta|=1$, we have first order upwinding, which is used at the device boundaries. When $|\delta|=0$, we have centered differencing. We apply an upwind bias only to T , the constant effective-mass drift term. The current density is defined to satisfy the discrete current continuity equation:

$$J_{j+1/2} = \frac{\hbar}{8N_k\Delta^2} \sum_n \left[\frac{\sin(2k_n\Delta) [(1\pm\delta)f_{j+1n} + (1\mp\delta)f_{jn}]}{m_{GaAs}^*} + \frac{1}{N_k} \sum_{n'} \sin(2k_{n'}\Delta) [M_{j+1n-n'}^e f_{j+1n'} + M_{jn-n'}^e f_{jn'}] \right]$$

The top sign is used for $k < 0$ and the bottom sign for $k > 0$. Since $V(q, k-k')$ strongly couples the upwind and downwind flows, the fact that the differencing in eq. 3 is not transportive should not be of major concern. In any case, the exact equation of motion is not transportive either.

Simulation Results

The above model is first applied to the most commonly simulated $\text{Al}_{0.3}\text{Ga}_{0.7}\text{As}/\text{GaAs}$ resonant-tunneling diodes [1, 3, 4]. The conduction band offset is 0.27eV, $m_{GaAs}^* = 0.067m_0$, and $m_{AlGaAs}^* = 0.092m_0$. 30Å barriers sandwich a 50 Å well. The applied bias is dropped linearly across the double barrier quantum well structure. The contact is doped n-type at $2 \times 10^{18} \text{ cm}^{-3}$. Figure 1 shows the flat-band results. The results due to Tsuchiya *et al.* [1] are also shown.

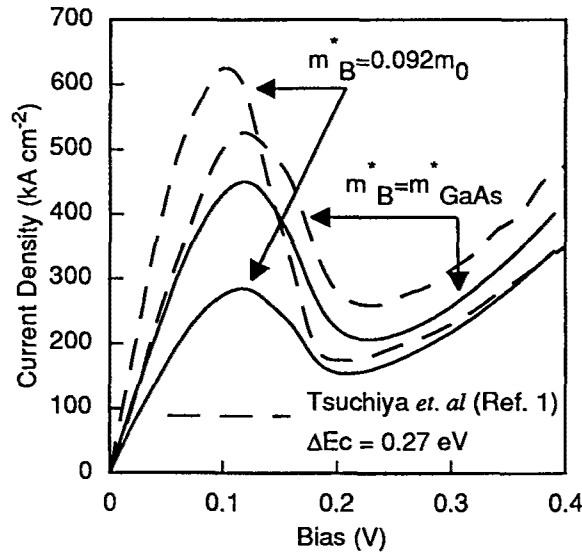


Figure 1: Wigner conduction curves with first order upwinding for $\text{Al}_{0.3}\text{Ga}_{0.7}\text{As}/\text{GaAs}$ diode. Collisions are ignored. $N_q = 80$, $\Delta = a$, $N_k = 64$ as in [1]. Solid lines: our model, dashed lines: Tsuchiya *et al.* [1]. The current density should decrease with increasing effective-mass in the barriers.

$\text{AlAs}/\text{InGaAs}$ or AlAs/GaAs diodes are the choice for high speed applications due to their high peak current densities and peak-to-valley ratios [5-7]. The inadequacy of the first order upwinding begins to surface as we attempt to simulate AlAs/GaAs resonant-tunneling diodes. Here we consider our baseline AlAs/GaAs resonant-tunneling diode. The conduction band offset is taken to be 1.0eV, $m^*\text{GaAs}=0.067m_0$, and $m^*\text{AlAs}=0.15m_0$. 17 Å barriers sandwich a 50 Å well. On either side of the tunneling structure is a three step spacer layer consisting of 50 Å undoped GaAs

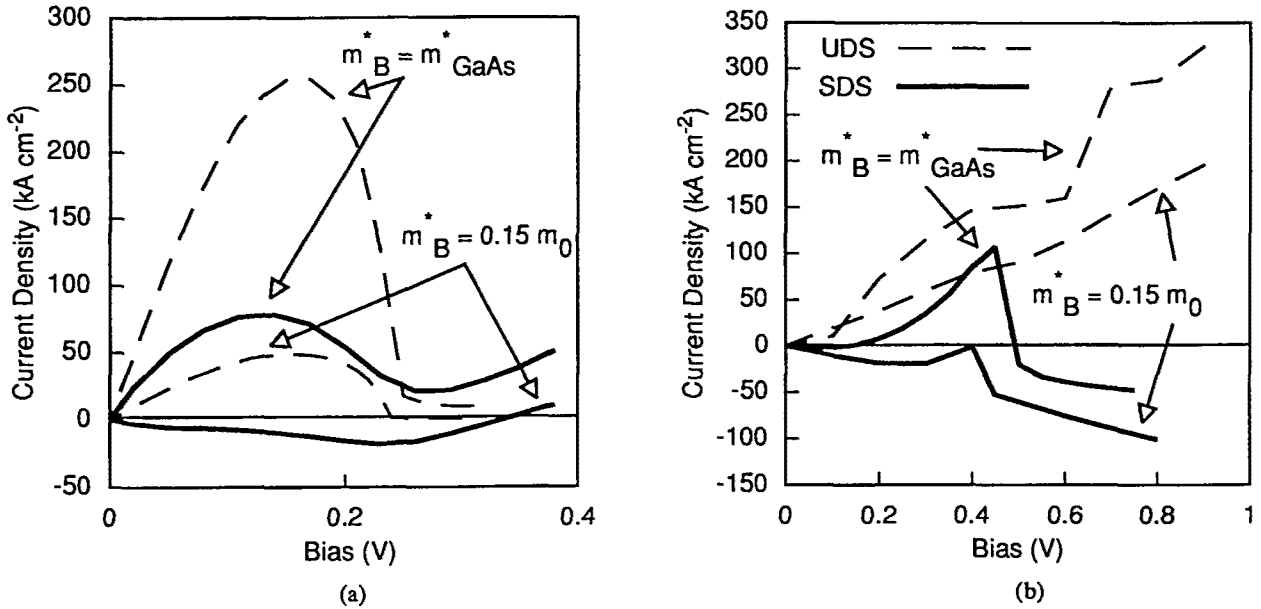


Figure 2: Conduction curves for AlAs/GaAs diode a) heavy lines: flat-band Wigner curves using first order upwinding. Schrödinger curves are shown as light dashed lines. b) self-consistent curves. The heavy lines are Wigner curves using second order upwinding (SDS), the light dashed lines using first order upwinding (UDS). Collisions are ignored. $N_q = 268$, $\Delta = a$, $N_k = 128$ in the Wigner calculations. The results are far from being satisfactory. Increasing N_k to 256 led to similar results. $\Delta = a/2$, $N_q = 536$, $N_k = 256$ does not help either.

closest to the barriers, 100 Å, $5 \times 10^{16} \text{ cm}^{-3}$ n-type GaAs and 100 Å, $6 \times 10^{17} \text{ cm}^{-3}$ n-type GaAs. The contact regions are $4 \times 10^{18} \text{ cm}^{-3}$ n-type GaAs. Figure 2a shows the Wigner conduction curves using

first order upwinding under flat-band conditions. For comparison the Schrödinger results are also shown. Figure 2b shows the self-consistent (potential is self-consistent to within 10^{-4} eV) Wigner conduction curves obtained by using first and second order upwinding. Flat-band, constant mass calculations have been reported for InGaAs/AlAs diodes using first order upwinding [8] and as can be seen from fig. 2a, under such conditions, the problems with the approach are not obvious.

To improve the fidelity of the numerical model to the exact equation, we use $|\delta| = 0.1$ in eq. 3. The resulting curves are shown in fig. 3a. The improvement over the other approaches is remarkable. For comparison, the Schrödinger-Poisson curves are also shown. Finally, including collisions in the relaxation time approach ($\tau = 100$ fs) and using $|\delta| = 0.01$, the simulated and measur-

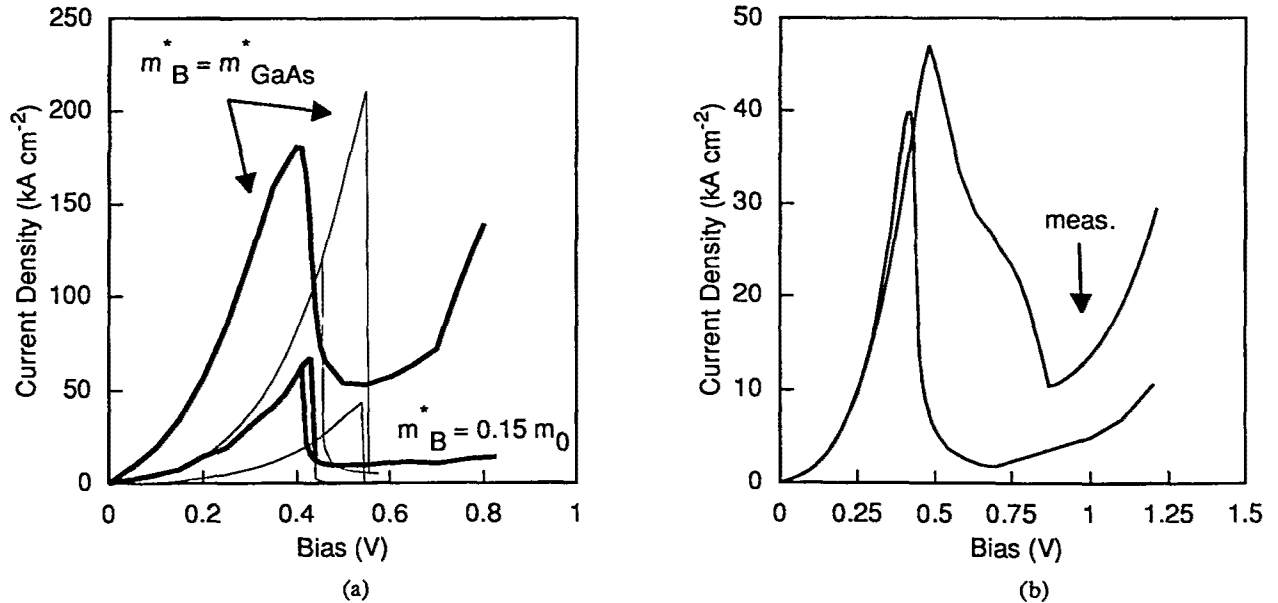


Figure 3: Improved Wigner conduction curves for AlAs/GaAs diode. a) heavy lines show the Wigner-Poisson results (collision free, $|\delta| = 0.1$) and the light lines are due to the Schrödinger-Poisson model. b) $\tau = 100$ fs, $|\delta| = 0.01$. $N_q = 268$, $\Delta = a$, $N_k = 128$. Also shown is a typical measured curve (300K) for our baseline.

ed curves are compared in fig. 3b. The poor agreement beyond the peak is an unresolved problem and has been the subject of intense discussions.

In conclusion, self-consistent steady state conduction curves for GaAs/AlAs resonant-tunneling diodes have been presented for the first time. The inclusion of the higher effective-mass in AlAs is essential. A new approach to obtaining meaningful conduction curves has been proposed and leads to much improved results.

Calculations were done on IBM RS/6000 models 590 and 320H. This work was sponsored in part by the Joint Services Electronics Program under Grant No. AFOSR 49620-92-C-0027, and by the Air Force Office of Scientific Research under AASERT Grant No. AFOSR F49620-93-1-0479.

References

1. H. Tsuchiya, M. Ogawa, and T. Miyoshi, *IEEE Trans. Electron Devices*, **38**, 1246 (1991).
2. S. R. De Groot, and L. G. Suttrop, *Foundations of Electrodynamics*. North-Holland, 1972.
3. F. A. Buot, and K. L. Jensen, *Physical Review*, **B 42**, 9429 (1990).
4. W. R. Frensley, *Reviews of Modern Physics*, **62**, 745 (1990).
5. D. H. Chow, J. N. Schulman, E. Ozbay, and D. M. Bloom, *Appl. Phys. Lett.*, **61**, 1685 (1992).
6. V. K. Reddy, A. J. Tsao, and D. P. Neikirk, *Electronics Lett.*, **26**, 1742 (21 1990).
7. T. P. E. Broekaert, and C. G. Fonstad, *IEDM Technical Digest*, 559 (1989).
8. R. K. Mains, and G. I. Haddad, *Journal of Applied Physics*, **64**, 5041 (10 1988).